Accepted Manuscript

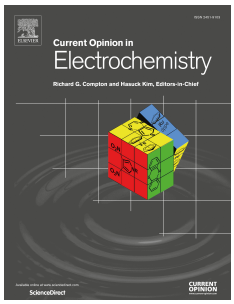

Recent Advances In The Development Of Electrochemical Hydrogen Peroxide Carbon Nanotubes-Based (Bio)Sensors

M. Eguílaz, P.R. Dalmasso, M.D. Rubianes, F. Gutierrez, M. Rodríguez, P. Gallay, M.López Mujica, M.L. Ramírez, C. Tettamanti, A. Montemerlo, G.A. Rivas

PII: S2451-9103(18)30280-1

DOI: https://doi.org/10.1016/j.coelec.2019.02.007

Reference: COELEC 371

To appear in: *Current Opinion in Electrochemistry*

Received Date: 21 December 2018

Revised Date: 25 February 2019

Accepted Date: 26 February 2019

Please cite this article as: Eguílaz M, Dalmasso PR, Rubianes MD, Gutierrez F, Rodríguez M, Gallay P, Mujica ML, Ramírez ML, Tettamanti C, Montemerlo A, Rivas GA, Recent Advances In The Development Of Electrochemical Hydrogen Peroxide Carbon Nanotubes-Based (Bio)Sensors, *Current Opinion in Electrochemistry*, https://doi.org/10.1016/j.coelec.2019.02.007.

RECENT ADVANCES IN THE DEVELOPMENT OF ELECTROCHEMICAL HYDROGEN PEROXIDE CARBON NANOTUBES-BASED (BIO)SENSORS

M. Eguílaz[1,*], P. R. Dalmasso[2,*], M. D. Rubianes[1], F. Gutierrez[1], M. Rodríguez[1], P. Gallay[1], M. López Mujica[1], M. L. Ramírez[1], C. Tettamanti[1], A. Montemerlo[1], G. A. Rivas[1,*]

[1]INFIQC, CONICET, Departamento de Fisicoquímica, Facultad de Ciencias Químicas, Universidad Nacional de Córdoba. Ciudad Universitaria, 5000-Córdoba. Argentina.

[2]CIQA, Departamento de Ingeniería Química, Facultad Regional Córdoba, Universidad Tecnológica Nacional. Maestro López esq. Cruz Roja Argentina, 5016-Córdoba, Argentina.

***Corresponding authors: mrubio@fcq.unc.edu.ar; p-dalmasso@hotmail.com; grivas@fcq.unc.edu.ar**

Abstract

The relevance of H_2O_2 as biomarker for different neurodegenerative diseases and cancer has been one of the most significant incentives for the development of new (bio)sensors that allow a more sensitive, selective, fast, and stable quantification of H_2O_2. In this regard, the association of carbon nanotubes with hemoproteins, nanoparticles, and other nanostructures and different electrochemical transducers, has offered new avenues for the construction of innovative H_2O_2 bioanalytical platforms. This short review highlights the most relevant contributions in the field of electrochemical (bio)sensors for H_2O_2 based on carbon nanotubes published in the period 2016-2018.

Introduction

Hydrogen peroxide is a compound of great importance in different fields. It is a product of several metabolic routes [1,2] and high levels may produce diseases connected with oxidative stress like cancer, cardiovascular disorders and Alzheimer disease [3-7]. The concentrations go from nM to μM depending on the fluid and cell-type [2]. Due to their oxidative properties, H_2O_2 has been also used for the synthesis of organic compounds, pulp and paper bleaching, sterilization, clinical and pharmaceutical applications [8,9].

Several sensing methodologies have been proposed for the quantification of H_2O_2 [10-13], new analytical platforms that allow the fast, highly sensitive and selective quantification are highly required. Electrochemical sensors have demonstrated to be very useful for the quantification of different analytes [14-20] and H_2O_2 hydrogen peroxide in particular [17-20]. There are two types of H_2O_2 electrochemical sensors, the enzymatic ones, based on the use of biocatalysts (heme-proteins) [17,18] and the non-enzymatic ones, based on the use of different catalytic (nano)materials [19,20]. The enzymatic biosensors demonstrated to be a very interesting alternative for the quantification of H_2O_2; however, they have some drawbacks associated with the cost and instability of the enzymes. Consequently, the development of non-enzymatic strategies for the quantification of hydrogen peroxide is currently a very hot topic.

In this short review, we discuss the most relevant electrochemical sensing strategies for H_2O_2 based on the use of carbon nanotubes (CNTs) developed in the period 2016-2018 (Figure 1). CNTs are allotropes of carbon that consist of a

graphene sheet rolled into a tube [21,22] either defining a cylinder (single-walled carbon nanotubes, SWCNTs) or concentric and closed tubules (multi-walled carbon nanotubes, MWCNTs) [23]. Due to their unique properties of CNTs [24-28], the incorporation of CNTs in these (bio)sensors presents several advantages: facilitates the charge transfer and/or increases the surface area, and/or enables the anchoring of different (bio)molecules and/or improves the conductivity of the resulting platform. The working potential to quantify H_2O_2 in a sensitive and selective way is a key point. However, the reduction of H_2O_2 requires, in general, negative potentials to obtain a sensitive response, making necessary a rigorous desoxygenation of the buffer, standard solutions and samples to avoid the interference of oxygen reduction. On the other hand, for the oxidation of H_2O_2 is necessary to work at very positive potentials and under these conditions, the interference of easily oxidizable compounds usually present in biological fluids or in foods samples is a critical problem. In these cases, the presence of nanostructures is very important to decrease the overvoltages. Table 1 summarizes the most relevant analytical parameters and experimental conditions for the different H_2O_2 electrochemical (bio)sensors discussed in the review.

H_2O_2 electrochemical sensors based on the association of CNTs and hemoproteins

Eguílaz et al. [29**] reported the non-covalent functionalization of MWCNTs with cytochrome c (Cyt c) and the highly sensitive and selective H_2O_2 biosensing using a glassy carbon electrode (GCE) modified with MWCNTs-Cyt c. The close interaction of MWCNTs with Cyt c and the efficient biocatalytic activity of the

hemeprotein that supports the MWCNTs, made possible the efficient amperometric response for H_2O_2 at –0.100V from the direct electron transfer (DET) of Cyt c. A linear range from $1.0x10^{-6}$ to $1.6x10^{-4}$M, a sensitivity of (43±1) $mAM^{-1}cm^{-2}$, a limit of detection (LOD) of $1.5x10^{-7}$M, and very good repeatability, reproducibility and long-term stability were reported for this biosensor. It was successfully used to quantify H_2O_2 in mouthwash and enriched low-fat milk samples. Aghamiri et al. [30] discussed the advantages of the immobilization of Cyt c at GCE modified with a porous and conductive thin-film of electropolymerized polyaniline(PANI)/MWCNTs. The immobilization of the enzyme in the net of the polymer-CNTs facilitated the DET of the iron center and the quantification of H_2O_2 was successfully performed at submicromolar levels from amperometric measurements at –0.400V. It is important to mention that, as in the case of other pseudoperoxidases, the absence of the sixth axial heme-ligand in cytochrome *c* is essential to bind H_2O_2 and catalyze its reduction [31].

Alim et al. [32] proposed a very sensitive third-generation H_2O_2 biosensor based on the immobilization of multiporous SnO_2 nanofiber (SnO_2NFs), MWCNTs, and hemoglobin (Hb) at GCE by using chitosan (CS). The proposed architecture allowed the DET of the protein metallic center and, consequently, the amperometric detection of H_2O_2 at –0.400V at nanomolar levels. Another interesting sensing strategy for the nanomolar detection of H_2O_2 was based on a 3D bis-aniline-crosslinked network of 4-aminothiophenol-modified horseradish peroxidase (HRP) and aniline-modified SWCNTs at a 4-aminothiophenol self-assembled monolayer (SAM)-modified gold electrode [33]. An original approach was described by Draminska and Bilewickz [34] who proposed a bienzymatic

biosensor based on the use of a nanocomposite integrated by MWCNTs, catalase and laccase or bilirubin oxidase cross-linked with glutaraldehyde (GAD). Catalase transforms the H_2O_2 into oxygen and water and the multi-copper enzymes catalyze the reduction of the enzymatically generated oxygen to water. The sensor was successfully used to quantify H_2O_2 in different pharmaceutical formulations. The strategy is interesting although the analytical performance is not as competitive as the previous ones.

Another innovative and competitive alternative involving a catalytic center that mimics the active site of hemoproteins was presented by Wu et al. [35**]. They reported the non-covalent immobilization of hemin, an iron(III)protophorphyrin IX, at MWCNTs using tetraoctylammonium bromide (TOAB) to provide the cations necessary to bind to the carboxyl groups of hemin and MWCNTS, reducing, in this way, the electrostatic repulsion of hemin and MWCNTs carboxylic groups, and preventing the aggregation of the nanomaterials. The resulting platform allowed the quantification of H_2O_2 between 0.82 and 278.6µM, with a LOD of 0.26µM and a stability up to 11 days.

In general, the enzymatic biosensors allow a sensitive quantification of H_2O_2, and the overall performance is highly dependent on the efficiency of the hemoprotein immobilization, being the robustness and the intimate contact with the carbon nanostructures, key aspects to ensure a competitive analytical device. The presence of CNTs at the electrode surfaces allows a more efficient DET and the incorporation of higher amounts of enzyme, largely improving the analytical performance of the resulting biosensors compared to their counterparts of graphite, as it have been already demonstrated by Gorton et al. [36, 37].

H_2O_2 electrochemical sensors based on the association of metallic nanoparticles and CNTs

In the last years, the association of metallic nanoparticles (NPs) with CNTs have demonstrated to be an advantageous alternative for developing highly sensitive and selective H_2O_2 sensing [19, 20, 38-45].

Joshi et al. [39] addressed the need for a highly sensitive H_2O_2 microsensor able to be used in scanning electrochemical microscopy to simultaneously perform the approach curves and detect low levels of H_2O_2 in complex matrixes like bacterial biofilms. The sensor was obtained by electrodeposition of PtNPs at oxidized-MWCNTs and mixing with the 1-butyl-4-methylpyridinium hexafluorophosphate ionic liquid (IL) (Figure 2). The LOD was 250nM and the sensor allowed to obtain a 3D distribution of the H_2O_2 produced by a bacterial biofilm.

Hamidi and Haghighi [40] reported the modification of GCEs with a nanocomposite of PdNPs and MWCNTs dispersed in dimethylformamide (DMF). The catalytic activity of PdNPs largely improved the response of the sensor and allowed the fast and reproducible quantification of H_2O_2 either at 0.350V or at –0.250V, with LODs of 1.2 and 14µM, respectively. Zhang et al. [41*] presented an interesting flexible nanohybrid microelectrode based on the use of carbon fiber (CF), an excellent flexible substrate due to its small size and elasticity modulus, modified with highly ordered nitrogen doped CNTs arrays (N-CNTAs) decorated with AuNPs. The synergistic catalytic activity of N-CNTAs and AuNPs allowed to obtain a fast, stable and reproducible analytical signal at –0.300V, with LOD at

nanomolar levels, and successful application for sensing the H_2O_2 secreted from MCF-7 and MDA-MB-231 cells without the influence of bending-induced mechanical stress. Taking advantage of the inkjet printing potential, Shamkhalichenar and Choi [42*] introduced disposable and fast H_2O_2 sensors obtained by inkjet printing of a MWCNTs-based ink on paper followed by the incorporation of AgNPs to catalyze the reduction of H_2O_2.

The association of two or more catalytic centers demonstrated to be very useful to improve the analytical characteristics of electrochemical sensors. Ko et al. [43] demonstrated an interesting synergism by incorporating Au and Ag NPs in addition to SWCNTs. The sensing was performed at –0.150V in nitrogen-saturated solutions, with a LOD of 0.3µM and a very wide linear range, demonstrating the advantages of the presence of CoNPs in addition to PdNPs.

Heli et al. [45] proposed the use of a carbon paste modified with hexagonal Co-Al-layered double hydroxide nanoshales (CoAlLDH) and MWCNTs synthesized by reflux heating. The resulting sensor was successfully used to quantify H_2O_2 either at 0.230V or at –0.350V with LODs of 5 and 10µM, respectively.

The comparative analysis of the different strategies clearly indicates that the selection of the metallic center/s, the strategy to incorporate them to the transducer surface and the efficiency of the interaction with the carbon nanostructures are the most critical aspect for the development of H_2O_2 electrochemical sensors based on the use of metallic nanoparticles and CNTs.

H_2O_2 electrochemical sensors based on CNTs associated with other nanostructures

Bai et al. [46] presented an innovative work based on GCEs modified with a nanocomposite of carbon dots (CDs) and oxidized-MWCNTs. The good electrical conductivity and huge surface area of MWCNTs, their electron acceptor characteristics and the excellent donor capacity of CDs made possible the construction of an electrode with high electrocatalytic activity and notable synergism. MWCNTs:CDs ratio was very important for the analytical performance of the sensor, being 10:1 the selected one. A fast and stable response, with a linear range between $3.5x10^{-6}$ and $3.0x10^{-4}$M, a LOD of 0.25µM and a successful application for the quantification of the H_2O_2 released from HeLa cells and the H_2O_2 present in enriched human serum samples was also reported.

The use of MnO_2 as catalytic center for building H_2O_2 sensors has received great attention [47-50]. Begum et al. [47] reported the analytical performance of GCEs modified with a δ-MnO_2/MWCNTs nanocomposite obtained by one-step hydrothermal process in alkaline medium, where MnO_2 worked as electrocatalyst and MWCNTs was the responsible for the improvement of the platform conductivity. The resulting electrode made possible the fast, selective and reproducible detection of H_2O_2 at -0.300V in Ar saturated-0.1 M PBS solution with a detection limit of 1µM. Recoveries between 98 and 102% were reported in tomato sauce and tap water samples.

An innovative platform was obtained by the modification of GCE with a rGONR/MnO_2 nanocomposite obtained by one-step hydrothermal co-reduction of $KMnO_4$ and GONR (generated from the unzipping of MWCNTs) using citric acid [50*]. The resulting sensor showed an excellent analytical response at 0.800V in

PBS pH 7.4 due to the important synergistic catalytic activity of MnO_2/rGONRs for the oxidation of H_2O_2 and the high surface area and excellent conductivity of rGONR (Figure 3). The sensor allowed the detection of nanomolar levels of H_2O_2 and its quantification in a fetal bovine serum.

Shahnavaz and Hamid [51] proposed the submicromolar detection of H_2O_2 at –0.65 V using an electrode modified with MWCNTs-$ZnCr_2O_4$NPs synthesized by a hydrothermal method and further calcination at 500 ℃. The resulting sensor presented a linear range between 50µM and 0.8mM and was successfully used for the quantification of H_2O_2 in lens cleaning solution.

A more elaborated architecture based on the modification of GCEs with a composite of Pt encapsulated in a sixth-generation poly(amidoamine) dendrimer with amine terminations (G6-NH_2 PAMAM dendrimer) covalently attached to carboxylated-CNTs, was reported by Liu et al. [52]. A fast, reproducible and stable response was obtained at –0.150V, with a linear range between 3 and 400µM, a LOD of 0.8µM, and a successful determination of H_2O_2 in MCF-7 cells.

Currently, metal-organic frameworks (MOF) are under intense investigation for building electrochemical sensors. Wang et al. [53] proposed the quantification of H_2O_2 in 0.1M NaOH at 0.500V using GCEs modified with a dispersion of Ni(II)-based MOFNPs anchored on CNTs by solvothermal method (Ni(II)-MOF/CNTs), covered by 2.5% Nafion, where Ni(II) was easily adsorbed at oxidized-CNTs through the oxygenated groups. A highly reproducible and fast response, with linear range between 0.01 and 51.6mM was obtained with the sensor.

Roushani et al. [54**] reported a sensitive analytical platform for the quantification of H_2O_2 based on a rational selection of the components: C_{60},

MWCNTs, CS, and 1-methyl-3-octylimidazoliniumtetrafluoroborate (IL) deposited at GCE; methylene blue (MB) deposited at the resulting platform; and Cu(II) preconcentrated through the coordination with MB. This CuNPs/MB/MWCNTs-C_{60}-CS-IL sensor presented advantages such as the large surface area, π-π conjugated bonds, good conductivity, and synergism between Cu(II) and MB, which accelerated the charge transfer and facilitated the reduction of H_2O_2 at –0.180V. Reproducible and repeatable signals were obtained between 0.2 and 4µM, with a LOD of 55nM. The sensor was used to quantify H_2O_2 in enriched serum samples with very good recoveries.

Layer-by-layer self-assembling of monolayers is another interesting alternative for the versatile design of different sensing platforms. In this direction, De Fátima Cardoso Soares et al. [55] proposed a strategy based on ITO modified by self-assembling of agar-SWCNTs, poly(allylamine hydrochloride)(PAH)-SWCNTs, and alizarin red S (ARS) as catalyst. The analytical signal was obtained by amperometry at –0.500V with a LOD of 0.15µM. Zhang et al. [56] reported another supramolecular strategy based on the self-assembling of 2,9,16,23-tetra[4-(N-methyl)pyridinyloxyl]-phtalocyanine cobalt (II) ($[TMPyPcCo]^{4+}$) and oxidized-MWCNTs at GCE through electrostatic interaction to obtain an interconnected assembly (($[TMPyPcCo]^{4+}$/MWCNTs)$_n$). The combination of $[TMPyPcCo]^{4+}$ and oxidized-MWCNTs without any inert polymer binders allowed to expose more active sites for electrocatalysis, aspect very important in the performance of the sensor at –0.250V. Wang et al. [57] proposed the use of oxygen-doped, nitrogen rich carbon nanoribons polymer (ONPCNRs) electrostatically bond to

poly(diallyldimethylammonium chloride) (PDDA)-modified SWCNTs. The nanocomposite showed an improved electrocatalytic activity due to the electron withdrawing ability of the N-atoms from the ONPCNRs which create net positive charge on the adjacent carbon atoms in the PDDA/SWCNTs plane. The sensor, prepared by dropping ONPCNR/SWCNTs-PDDA at GCE, allowed the submicromolar detection of H_2O_2 with stable response for 2 weeks and successful use for the detection of H_2O_2 in enriched ultra-high temperature milk.

Mayuri et al. [58] introduced a copper-bipyridyl complex immobilized at MWCNTs-Nafion modified-GCE as a bioinspired electrocatalytic molecular system (Figure 4). The 2,2´bipyridyl-complex was dropped at Nafion/MWCNTs-modified GCE and the copper center was finally immobilized at the resulting platform by cycling 40 times in a 2mM $CuSO_4$ solution. The flow injection analysis with amperometric detection at –0.200V presented a linear range between 1μM and 1mM and a submicromolar-LOD. The analytical applications of the sensor were demonstrated by determination of H_2O_2 in a cosmetic product.

Nasirizadeh et al. [59] proposed the use of a GCE modified with MWCNTs dispersed in DMF followed by cycling the potential in a solution of reactive blue 19 (RB), a quinone derivative that catalyzes the reduction of H_2O_2, and allowed the detection of submicromolar concentrations of H_2O_2. The sensor was successfully used for the quantification of H_2O_2 in fruit juices.

General conclusions and perspectives

This short review addresses the recent trends for H_2O_2 electrochemical (bio)sensing based on the use of CNTs. Special emphasis was given to the

discussion of i) the strategies used to build the (bio)sensor, ii) the nature of the (bio)catalytic center, iii) the origin of the analytical signal, and iv) the most relevant analytical characteristics of the (bio)sensors.

While the use of hemoproteins as biocatalytic centers has allowed to obtain a highly sensitive H_2O_2 biosensing, special attention should be given to build platforms with increased robustness and enhanced biocatalytic activity. H_2O_2 sensors based on the use of nanomaterials as catalytic centers has also demonstrated to be very competitive; however, it is necessary to design new schemes of synthesis and functionalization of nanomaterials to obtain platforms that allow a more sensitive and selective quantification of this analyte.

Future trends should be focused on i) the rational modification of peroxidases and peroxidases-like proteins to obtain biocatalysts with increased robustness and biocatalytic activity, ii) the one-step functionalization of CNTs with new catalytic nanomaterials and/or catalytic centers that mimics the active sites of peroxidases or proteins with peroxidase activity, iii) the one-step unzipping of CNTs and reduction of the resulting GONR to obtain an adequate balance of mono- and bidimensional carbon nanostructures with different functionalization, and iv) the development of new inks for screen- or inkjet-printing involving elements that make possible the preparation of more efficient H_2O_2 disposable (bio)sensors.

Acknowledgements

The authors thank CONICET (PIP 2014, PIP 2015), SECyT-UNC (2018-2021), and ANPCyT-FONCyT (PICT 2014-1663, 2016-1261, 2016-1306) for the financial support.

References and recommended reading

Papers of particular interest, published within the period of review, have been highlighted as:

**Paper of special interest*

***Paper of outstanding interest*

[1] B. Haliwell, M. V. Clement, L. H. Long, Hydrogen peroxide in the human body. FEBS Lett 486 (2000) 10-13.

[2] X. Chen, B. Su, Z. Cai, X. Chen, M. Oyama, PtPd nanodendrites supported on graphene nanosheets: a peroxidase-like catalyst for colorimetric detection of H_2O_2, Sens. Actuators B Chem. 201 (2014) 286–292.

[3] E.W. Miller, B.C. Dickinson, C.J. Chang, Aquaporin-3 mediates hydrogen peroxide uptake to regulate downstream intracellular signaling, Proc. Nat. Acad. Sci. USA 107 (2010) 15681–15687.

[4] C.C. Winterbourn, Reconciling the chemistry and biology of reactive oxygen species, Nat. Chem. Biol. 4 (2008) 278–286.

[5] T.J. Preston, W.J. Muller, G. Singh, Scavenging of extracellular H_2O_2 by catalase inhibits the proliferation of HER-2/Neu-transformed rat-1 fibroblasts through the induction of a stress response, J. Biol. Chem. 276 (2001) 9558–9564.

[6] M.A. Yorek, The role of oxidative stress in diabetes vascular and neural disease, Free. Radic. Res. 37 (2003) 471–480.

[7] J.P. Spencer, A. Jennet, O.I. Aruoma, C.E. Cross, R. Wu, B. Halliwell, Oxidative DNA damage in human respiratory tract epithelial cells. Time course in relation to DNA strand breakage, Biochem. Biophys. Res. Commun, 224 (1996) 17–22.

[8] W. Chen, S. Cai, Q.Q. Ren, W. Wen, Y.D. Zhao, Recent advances in electrochemical sensing for hydrogen peroxide: a review, Analyst 137 (2012) 49–58.

[9] C.R. Holkar, A.J. Jadhav, D.V. Pinjari, N.M. Mahamuni, A.B. Pandit, A critical review on textile wastewater treatments: possible approaches, J. Environ. Manage. 182 (2016) 351–366.

[10] P. Gimeno, C. Bousquet, N. Lassu, A.-F. Maggio, C. Civade, C. Brenier, L. Lempereur, High-performance liquid chromatography method for the determination of hydrogen peroxide present or released in teeth bleaching kits and hair cosmetic products, J. Pharm. Biomed. Anal. 107 (2015) 386–393.

[11] X. Huang, H. Zhou, Y. Huang, H. Jiang, N. Yang, S.A. Shahzad, L. Meng, C. Yu, Silver nanoparticles decorated and tetraphenylethene probe doped silica nanoparticles: a colorimetric and fluorometric sensor for sensitive and selective detection and intracellular imaging of hydrogen peroxide, Biosens. Bioelectron. 121 (2018) 236–242.

[12] J.N. Tiwari, V. Vij, K.C. Kemp, K.S. Kim, Engineered carbon-nanomaterial-based electrochemical sensors for biomolecules, ACS Nano 10 (2016) 46–80.

[13] D. Yu, P. Wang, Y. Zhao, A. Fan, Iodophenol-enhanced luminol chemiluminiscence and its application to hydrogen peroxide and glucose detection, Talanta 146 (2016) 655-661.

[14] E.T.S.G. da Silva, D.E.P. Souto, J.T.C. Barragan, J.F Giarola, A.C.M. de Moraes, L.T. Kubota, L.T. Electrochemical biosensors in point-of-care devices: recent advances and future trends, ChemElectroChem 4 (2017) 778–794.

[15] Y.-H. Wang, K.-J. Huang, X. Wu, Recent advances in transition-metal dichalcogenides based electrochemical biosensors: a review, Biosens. Bioelectron. 97 (2017) 305–316.

[16] L. Wang, J. Li, M. Feng, L. Min, J. Yang, S. Yu, Y. Zhang, X. Hu, Z. Yang, Perovskite-type calcium titanate nanoparticles as novel matrix for designing sensitive electrochemical biosensing, Biosens. Bioelectron. 96 (2017) 220–226.

[17] M.B. Gholivand, M. Khodadadian, Amperometric cholesterol biosensor based on the direct electrochemistry of cholesterol oxidase and catalase on a graphene/ionic liquid-modified glassy carbon electrode, Biosens. Bioelectron. 53 (2014) 472–478.

[18] R. Zhang, W. Chen, Recent advances in graphene-based nanomaterials for fabricating electrochemical hydrogen peroxide sensors, Biosens. Bioelectron. 89 (2017) 249–268.

376 [19] S. Chen, R. Yuan, Y. Chai, F. Hu, Electrochemical sensing of hydrogen
377 peroxide using metal nanoparticles: a review. Microchim. Acta 180 (2013)
378 15–32.
379 [20] R. Zhang, W. Chen., Recent advances in graphene-based nanomaterials for
380 fabricating electrochemical hydrogen peroxide Sensors. Biosens.
381 Bioelectron. 89 (2016) 249-268.
382 [21] M.S. Dresselhaus, G. Dresselhaus, A. Jorio, Unusual properties and
383 structure of carbon nanotubes, Annu. Rev. Mater. Res. 34 (2004) 247–278.
384 [22] E.N. Primo, F. Gutierrez, M.D. Rubianes, N.F. Ferreyra, M.C. Rodríguez,
385 M.L. Pedano, A. Gasnier, A. Gutierrez, M. Eguílaz, P. Dalmasso, G. Luque,
386 S. Bollo, C. Parrado, G.A. Rivas, Electrochemistry in one dimension:
387 applications of carbon nanotubes, in: R.C. Alkire, P.N. Bartlett, J. Lipkowski
388 (Eds.), Electrochemistry of Carbon Electrodes, Wiley-VCH Verlag GmbH &
389 Co. KGaA, Weinheim, 2015, pp 83–119.
390 [23] V. Georgakilas, J.A. Perman, J. Tucek, R. Zboril, Broad family of carbon
391 nanoallotropes: classification, chemistry, and applications of fullerenes,
392 carbon dots, nanotubes, graphene, nanodiamonds, and combined
393 superstructures, Chem. Rev. 115 (2015) 4744–4822.
394 [24] Z. Li, Z. Liu, H. Sun, C. Gao, Superstructured assembly of nanocarbons:
395 fullerenes, nanotubes, and graphene, Chem. Rev. 115 (2015) 7046–7177.
396 [25] L. Wang, M. Pumera, Electrochemical catalysis at low dimensional carbons:
397 graphene, carbon nanotubes and beyond – a review, Appl. Mater. Today 5
398 (2016) 134–141.

[26] G. A. Rivas, M. C. Rodríguez, M. D. Rubianes, F. A. Gutierrez, M. Eguílaz, P. R. Dalmasso, E. N. Primo, C. Tettamanti, M. L. Ramírez, A. Montemerlo, P. Gallay, C. Parrado, Carbon nanotubes-based electrochemical (bio)sensors for biomarkers, Applied Materials Today 9 (2017) 566-588.

[27] L. Kong, W. Chen, Carbon nanotube and graphene-based bioinspired electrochemical actuators, Adv. Mater. 26 (2014) 1025–1043.

[28] P. Yáñez-Sedeño, A. González-Cortés, L. Agüí, J.M. Pingarrón, Uncommon carbon nanostructures for the preparation of electrochemical immunosensors, Electroanalysis 28 (2016) 1679–1691.

[29] M. Eguílaz, A. Gutierrez, G.A. Rivas, Non-covalent functionalization of multi-walled carbon nanotubes with cytochrome c: enhanced direct electron transfer and analytical applications, Sens. Actuators B Chem. 225 (2016) 74-80.

** *This article highlights the importance of performing a critical study about the use of Cyt c in the double role of dispersing agent and biorecognition element, discusses the direct electron transfer of the iron center and the advantages of the intimate contact of the hemoprotein and the nanostructures for the sensitive quantification of hydrogen peroxide.*

[30] Z.S. Aghamiri, M. Mohsennia, H.-A. Rafiee-Pour, Fabrication and characterization of cytochrome c-immobilized polyaniline/multi-walled carbon nanotube composite thin film layers for biosensor applications, Thin Solid Films 660 (2018) 484–492.

[31] S. Casalini, G. Battistuzzi, M. Borsari, C. A. Bortolotti, G. Di Rocco, A. Ranieri, M. Sola, Electron Transfer Properties and Hydrogen Peroxide

Electrocatalysis of Cytochrome c Variants at Positions 67 and 80, J. Phys. Chem. B 114 (2010) 1698–1706.

[32] S. Alim, A.K.M. Kafi, R. Jose, M.M. Yusolf, J. Vejayan, Enhanced direct electron transfer of redox protein based on multiparous SnO_2 nanofiber-carbon nanotube nanocomposite and its application in biosensing, Int. J. of Biol. Macromol. 114 (2018) 1071–1076.

[33] A.K.M. Kafi, M. Naqshabandi, M.M. Yusoff, M.J. Crossley, Improved peroxide biosensor based on horseradish peroxidase/carbon nanotube on a thiol-modified gold electrode, Enzyme Microb. Technol. 113 (2018) 67–74.

[34] S. Dramińska, R. Bilewicz, Bienzymatic mediatorless sensing of total hydrogen peroxide with catalase and multi-copper enzyme co-adsorbed at CNT-modified electrodes, Sens. Actuators B Chem. 248 (2017) 493–499.

[35] H. Wu, T. Wei, X. Li, J. Yang, J. Zhang, S. Fan, H. Zhang, Synergistic-effect-controlled tetraoctylammonium bromide/multi-walled carbon nanotube@hemin hybrid material for construction of electrochemical sensor, J. Electrochem. Soc. 164 (2017) B147–B151.

** *This is an important contribution since it proposses the incorporartion of a catalytic center that mimics the active site of peroxidase and peroxidase-like proteins and allows a sensitive hydrogen peroxide sensor.*

[36] F. Chekin, L. Gorton, I. Tapsobea, Direct and mediated electrochemistry of peroxidase and its electrocatalysis on a variety of screen-printed carbon electrodes: amperometric hydrogen peroxide and phenols biosensor, Anal. Bioanal. Chem. 407 (2015) 439–446.

[37] J.L. Olloqui-Sariego, G.S. Zakharova, A.A. Poloznikov, J.J. Calvente, D.M. Hushpulian, L. Gorton, R. Andreu, Inter-protein coupling enhances the electrocatalytic efficiency of tobacco peroxidase immobilized at a graphite electrode, Anal. Chem. 87 (2015) 10807–10814.

[38] T.-C. Chou, K.-Y. Wu, F.-X- Hsu, C.-K. Lee, Pt-MWCNT modified carbon electrode strip for rapid and quantitative detection of H_2O_2 in food, J. Food Drug Anal. 26 (2018) 662–669.

[39] V.S. Joshi, J. Kreth, D. Koley, Pt-decorated MWCNTs-ionic liquid composite-based hydrogen peroxide sensor to study microbial metabolism using scanning electrochemical microscopy, Anal. Chem. 89 (2017) 7709–7718.

***** *This article represents and innovative strategy to design a dual SECM probe by coupling a miniaturized sensor based on the use of PtNPs/MWCNTs/IL with a Pt electrode for evaluating the 3D distribution of the hydrogen peroxide produced by a bacterial biofilm.*

[40] H. Hamidi, B. Haghighi, Fabrication of a sensitive amperometric sensor for NADH and H_2O_2 using palladium nanoparticles-multiwalled carbon nanotube nanohybrid, Mater. Sci. Eng. C Mater. Biol. Appl. 62 (2016) 423–428.

[41] Y. Zhang, J. Xiao, Y. Sun, L. Wang, X. Dong, J. Ren, W. He, F. Xiao, Flexible nanohybrid microelectrode based on carbon fiber wrapped by gold nanoparticles decorated nitrogen doped carbon nanotube arrays: in situ electrochemical detection in live cancer cells, Biosens. Bioelectron. 100 (2018) 453–461.

* *This is an interesting approach focused on the advantages of using a flexible substrate as platform for further immobilization of the different components with enormous potential.*

[42] H. Shamkhalichenar, J.-W. Choi, An inkjet-printed non-enzymatic hydrogen peroxide sensor on paper, J. Electrochem. Soc. 164 (2017) B3101–B3106.

* *The importance of this work comes from the innovation proposed to produce cheaper, versatile, and more reproducible sensing platforms.*

[43] E. Ko, V.-K. Tran, Y. Geng, W.S. Chung, C.H. Park, M.K. Kim, G.H. Jin, G.H. Seong, Continuous electrochemical detection of hydrogen peroxide by Au-Ag bimetallic nanoparticles in microfluidic devices, J. Electroanal. Chem. 792 (2017) 72–78.

[44] B. Huang, Y. Wang, Z. Lu, H. Du, J. Ye, One pot synthesis of palladium-cobalt nanoparticles over carbon nanotubes as a sensitive non-enzymatic sensor for glucose and hydrogen peroxide detection, Sens. Actuators B Chem. 252 (2017) 1016–1025.

[45] H. Heli, J. Pishahang, H. Barzegar Amiri, Synthesis of hexagonal CoAl-layered double hydroxide nanoshales/carbon nanotubes composite for the non-enzymatic detection of hydrogen peroxide, J. Electroanal. Chem. 768 (2016) 134–144.

[46] J. Bai, C. Sun, X. Jiang, Carbon dots-decorated multiwalled carbon nanotubes nanocomposites as a high-performance electrochemical sensor for detection of H_2O_2 in living cells, Anal. Bioanal. Chem. 408 (2016) 4705–4714.

[47] H. Begum, M.S. Ahmed, S. Jeon, A novel δ-MnO_2 with CNTs nanocomposites as enzyme-free sensor for hydrogen peroxide electrosensing, RSC Adv. 6 (2016) 50572–50580.

[48] K.K. Rani, R. Devasenathipathy, S.-F. Wang, C. Yang, Simple preparation of birnessite-type MnO_2 nanoflakes with multi-walled carbon nanotubes for the sensitive detection of hydrogen peroxide, Ionics 23 (2017) 3219–3226.

[49] S.-J. Li, J.-C. Zhang, J. Li, H.-Y. Yang, J.-J. Meng, B. Zhang, A 3D sandwich structured hybrid of gold nanoparticles decorated MnO_2/graphene-carbon nanotubes as high performance hydrogen peroxide sensors, Sens. Actuators B Chem. 260 (2018) 1–11.

[50] Z.-L. Wu, C.-K. Li, J.-G. Yu, X.-Q. Chen, MnO_2/reduced graphene oxide nanoribbons: facile hydrothermal preparation and their application on amperometric detection of hydrogen peroxide, Sens. Actuators B Chem. 239 (2017) 544–552.

* *This contribution is very interesting because it proposes a simple one-step synthesis of MNO_2/rGONR that allowed the determination of hydrogen peroxide at nanomolar level.*

[51] Z. Shahnavaz, S.B. Abd Hamid, Fabrication of a novel metal chromite-carbon nanotube composite for the highly efficient electrocatalytic reduction of hydrogen peroxide, Appl. Surf. Sci. 407 (2017) 379–385.

[52] J.-X. Liu, S.-N. Ding, Non-enzymatic amperometric determination of cellular hydrogen peroxide using dendrimer-encapsulated Pt nanoclusters/carbon

514 nanotubes hybrid composites modified glassy carbon electrode, Sens.
515 Actuators B Chem. 251 (2017) 200–207.
516 [53] M.-Q. Wang, Y. Zhang, S.-J. Bao, Y.-N. Yu, C. Ye, Ni(II)-based metal-
517 organic framework anchored on carbon nanotubes for highly sensitive non-
518 enzymatic hydrogen peroxide sensing, Electrochim. Acta 190 (2016) 365–
519 370.
520 [54] M. Roushani, K. Barkyas, B. Zare Dizajdizi, Development of sensitive
521 amperometric hydrogen peroxide sensor using a CuNPs/MB/MWCNT-C60-
522 Cs-IL nanocomposite modified glassy carbon electrode, Mater. Sci. Eng. C
523 Mater. Biol. Appl. 64 (2016) 54–60.
524 ** *This article represents a judicious design of a hydrogen peroxide sensing*
525 *platform to obtain a supramolecular architecture that allows the nanomolar*
526 *detection of hydrogen peroxide.*
527 [55] M. de Fátima Cardoso Soares, E.A. de Oliveira Farias, D.A. da Silva, C.
528 Eiras, Development and characterization of hybrid films based on agar and
529 alizarin red S for applications as non-enzymatic sensors for hydrogen
530 peroxide, J. Mater. Sci. 51 (2016) 7093–7107.
531 [56] J. Zhang, Z. Chen, H. Wu, F. Wu, C. He, B. Wang, Y. Wu, Z. Ren, An
532 electrochemical bifunctional sensor for the detection of nitrite and hydrogen
533 peroxide based on layer-by-layer multilayer films of cationic phthalocyanine
534 cobalt(II) and carbon nanotubes, J. Mater. Chem. B 4 (2016) 1310–1317.
535 [57] Z.-X. Wang, J.-Y. Wang, X.-H. Yu, F.-Y. Kong, W.-J. Wang, W.- X. Lv, L.
536 Ge, W. Wang, Synergistic contributions by decreasing overpotential and
537 enhancing electrocatalytic reduction in ONPCNRs/SWCNTs nanocomposite

538 for highly sensitive nonenzymatic detection of hydrogen peroxide, Sens.
539 Actuators B Chem. 246 (2017) 726–733.
540 [58] P. Mayuri, N. Saravanan, A.S. Kumar, A bioinspired copper 2,2-bipyridyl
541 complex immobilized MWCNT modified electrode prepared by a new
542 strategy for elegant electrocatalytic reduction and sensing of hydrogen
543 peroxide, Electrochim. Acta, 240 (2017) 522–533.
544 [59] N. Nasirizadeh, Z. Shekari, A. Nazari, M. Tabatabaee, Fabrication of a novel
545 electrochemical sensor for determination of hydrogen peroxide in different
546 fruit juice samples, J. Food Drug Anal. 24 (2016) 72–82.
547

Table 1: Analytical performance of the most relevant hydrogen peroxide electrochemical (bio)sensors reported in the period 2016-2018.

Hydrogen peroxide electrochemical sensors based on the association of CNTs and hemoproteins						
Platform	***Sensitivity***	***Detection***	***Linear Range***	***LOD***	***Sample***	***Ref.***
GCE/MWCNTs-Cyt c	(43 ± 1) mA M^{-1} cm^{-2}	Amp. (-0.100 V)	1.0 x 10^{-6} – 1.6 x 10^{-4} M	0.15 µM	Mouthwash and low-fat milk samples	[29]
GCE/MWCNTs/PANI/Cyt c	3108 nA μM^{-1} cm^{-2}	Amp. (-0.400 V)	2.0 x 10^{-6} – 6.0 x 10^{-4} M	0.2 µM	--	[30]
GCE/SnO_2NFs-MWCNTs-Hb-CS	--	Amp. (-0.400 V)	1.0 x 10^{-6} – 1.4 x 10^{-4} M	0.03 µM	--	[32]
AuE/SAM/SWCNTs/HRP	0.34 µA μM^{-1}	Amp. (-0.400 V)	1.2 x 10^{-7} – 1.2 x 10^{-4} M	0.022 µM	--	[33]
a. GCE/MWCNTs/GAD/Lac-Cat b. GCE/MWCNTs/GAD/BOx-Cat	a. 335.31 µA mM^{-1} cm^{-2} b. 263.46 µA mM^{-1} cm^{-2}	a. Amp. (+0.200 V) b. Amp. (+0.200 V)	a. 3 x 10^{-5} – 6.2 x 10^{-4} M b. 5 x 10^{-5} – 9.9 x 10^{-4} M	a. 33.1 µM b. 54.4 µM	Pharmaceutical formulations	[34]
Hydrogen peroxide electrochemical sensors based on the association of metallic nanoparticles and CNTs						
Platform	***Sensitivity***	***Detection***	***Linear Range***	***LOD***	***Sample***	***Ref.***
GCE/MWCNTs-TOAB-Hemin	1.37 µA μM^{-1} cm^{-2}	Amp. (+0.940 V)	8.2 x 10^{-7} M – 2.786 x 10^{-4} M	0.26 µM	--	[35]
SPCE/MWCNTs-PtNPs	142.8 µA mM^{-1} cm^{-2}	Amp. (+0.300 V)	1.0 x 10^{-5} – 1.0 x 10^{-4} M	10 µM	Green tea and pressed tofu samples	[38]
Pt-UME/MWCNTs-PtNPs-IL	(2.4 ± 0.24) mA mM^{-1} cm^{-2}	CV (+0.500 V)	1.0 x 10^{-5} M – 5 x 10^{-4} M	0.25 µM	Bacterial biofilms and saliva samples	[39]
GCE/MWCNTs-PdNPs	Oxidation: 167 µA mM^{-1} cm^{-2} Reduction: 68 µA mM^{-1} cm^{-2}	Amp. (Oxidation: +0.350 V and reduction: -0.250 V)	Oxidation: 2.0 x 10^{-6} – 6.0 x 10^{-5} M Reduction: 2.0 x 10^{-5} – 1.0 x 10^{-3} M	Oxidation: 1.2 µM Reduction: 14 µM	--	[40]
CF@N-CNTAs–AuNPs	142 µA mM^{-1} cm^{-2}	Amp. (-0.300 V)	Up to 4.3 x 10^{-3} M	0.05 µM	Breast cancer cells	[41]
IPMWCNTsE/AgNPs	--	Amp. (-0.300 V)	1.0 x 10^{-6} – 7.0 x 10^{-4} M	--		[42]
GS/SWCNTs/Au-AgNPs	13.1 µA mM^{-1} cm^{-2}	CV (-0.400 V)	3 x 10^{-4} M – 1.8 x 10^{-3} M	26.8 µM	Commercial antiseptic solutions	[43]
GCE/Pd-Co-CNTs	101.712 µA mM^{-1}	Amp. (-0.150 V)	1 x 10^{-6} M – 1.11 x 10^{-3} M	0.3 µM	--	[44]
CPE(CoAlLDH-MWCNTs)	Oxidation: 118 mA M^{-1} cm^{-2} Reduction: 42 mA M^{-1} cm^{-2}	Amp. (Oxidation: +0.230 V and reduction: -0.350 V)	Oxidation: 1 x 10^{-4} M – 4 x 10^{-3} M Reduction: 1 x 10^{-4} M – 4 x 10^{-3} M	Oxidation: 5 µM Reduction: 10 µM	River and wastewater samples	[45]
Hydrogen peroxide electrochemical sensors based on the association of CNTs and associated with other nanostructures						
Platform	***Sensitivity***	***Detection***	***Linear Range***	***LOD***	***Sample***	***Ref.***
GCE/oMWCNTs-CDs	0.039 µA μM^{-1}	Amp. (-0.180 V)	3.5 x 10^{-6} M – 3.0 x 10^{-4} M	0.25 µM	Human serum samples and HeLa cells	[46]
GCE/delta- δ -MnO_2/MWCNTs	243.9 µA mM^{-1} cm^{-2}	Amp. (-0.300 V)	5 x 10^{-5} M – 2.2 x 10^{-2} M	1 µM	Tomato sauce and tap water	[47]
GCE/f-MWCNTs-MnO_2NFs	219.05 µA mM^{-1} cm^{-2}	Amp. (-0.400 V)	5 x 10^{-6} M – 4.53 x 10^{-3} M	0.952 µM	Clinical lens solutions	[48]
GCE/rGONRs-MnO_2/AuNPs	452 µA mM^{-1} cm^{-2}	Amp. (+0.400 V)	4 x 10^{-7} M – 6.268 x 10^{-4} M	0.1 µM	Disinfectant	[49]

					and human serum samples	
GCE/rGONRs/MnO_2	0.0142 μA μM^{-1}	Amp. (+0.800 V)	2.5 x 10^{-7} M – 2.245 x 10^{-3} M	0.071 μM	Fetal bovine serum	[50]
GCE/MWCNTs-$ZnCr_2O_4$NPs	1717 μA mM^{-1} cm^{-2}	Amp. (-0.650 V)	5 x 10^{-5} M – 8 x 10^{-4} M	0.11 μM	Clinical lens solutions	[51]
GCE/CNTs-PAMAM DENs-PtNCs	987.5 μA $mM^{-1}cm^{-2}$	Amp. (-0.150 V)	3 x 10^{-6} M – 4 x 10^{-4} M	0.8 μM	Breast cancer cells	[52]
GCE/CNTs-Ni(II)-MOF	8.2 μA mM^{-1}	Amp. (+0.500 V)	1 x 10^{-5} M – 5.16 x 10^{-2} M	2.1 μM	--	[53]
GCE/C_{60}-MWCNTs-CS-IL/MB/CuNPs	0.0243 μA μM^{-1}	Amp. (-0.180 V)	2 x 10^{-7} M – 4 x 10^{-6} M	0.055 μM	Human blood serum samples	[54]
ITO/SWCNTs-agar/SWCNTs-PAH/ARS	--	Amp. (-0.500 V)	--	0.15 μM	--	[55]
GCE/$([TMPyPcCo]^{4+}$/oMWCNTs$)_{12}$	1.61028 μA mM^{-1}	DPV (-0.250 V)	1 x 10^{-5} M – 9 x 10^{-3} M	2.8 μM	Tap wáter samples	[56]
GCE/SWCNTs-PDDA-ONPCNRs	--	Amp. (-0.200 V)	--	0.51 μM	UHT milk samples	[57]
GCE/MWCNTs-Nafion/bpy/Cu^{2+}	96 nA μM^{-1} cm^{-2}	Amp. (-0.200 V)-FIA	1 x 10^{-6} M – 1 x 10^{-3} M	0.49 μM	Cosmetic cream samples	[58]
GCE/MWCNTs/RB	0.0086 μA μM^{-1}	Amp. (-0.300 V)	1 x 10^{-6} M – 2.8 x 10^{-5} M	0.27 μM	Fruit juice samples	[59]

GCE: glassy carbon electrode; MWCNTs: multi-walled carbon nanotubes; Cyt c: cytochrome c; PANI: polyaniline; SnO_2NFs: multiporous nanofiber of SnO_2; Hb: hemoglobin; CS: chitosan; AuE: gold electrode; SAM: 4-aminothiophenol self-assembled monolayer; SWCNTs: single-walled carbon nanotubes; HRP: horseradish peroxidase; GAD: glutaraldehyde; Lac: laccase; Cat: catalase; BOx: bilirubin oxidase; SPCE: screen-printed carbon electrode; PtNPs: platinum nanoparticles; Pt-UME: platinum ultramicroelectrode; IL: ionic liquid; PdNPs: palladium nanoparticles; CF: carbon fiber; N-CNTAs: nitrogen doped carbon nanotube arrays; AuNPs: gold nanoparticles; IPMWCNTsE: inkjet-printed multi-walled carbon nanotubes electrode; AgNPs: silver nanoparticles; GS: glass substrate; Au-AgNPs: gold-silver bimetallic nanoparticles; Pd-Co-CNTs: palladium-cobalt nanoparticles over carbon nanotubes; CPE: carbon paste electrode; CoAlLDH: Co-Al-layered double hydroxide nanoshales; oMWCNTs: oxidized multi-walled carbon nanotubes; CDs: carbon dots; MnO_2NFs: manganese oxide nanoflakes; rGONRs: reduced graphene oxide nanoribbons; $ZnCr_2O_4$NPs: zinc chromite nanoparticles; PAMAM DENs: poly(amidoamine) dendrimers; PtNCs: platinum nanoclusters; MOF: metal-organic framework; C_{60}: fullerene; MB: methylene blue; CuNPs: copper nanoparticles; ITO: indium tin oxide; PAH: poly(allylamine hydrochloride); ARS: alizarin red S; $[TMPyPcCo]^{4+}$: 2,9,16,23-tetra[4-(N-methyl) pyridinyloxy] phthalocyanine cobalt (II); PDDA: poly(diallyldimethylammonium chloride); ONPCNRs: oxygen doped, nitrogen-rich carbon nanoribbons polymer; TOAB: tetraoctylammonium bromide; bpy: 2,2´-bipyridyl; RB: reactive blue 19.

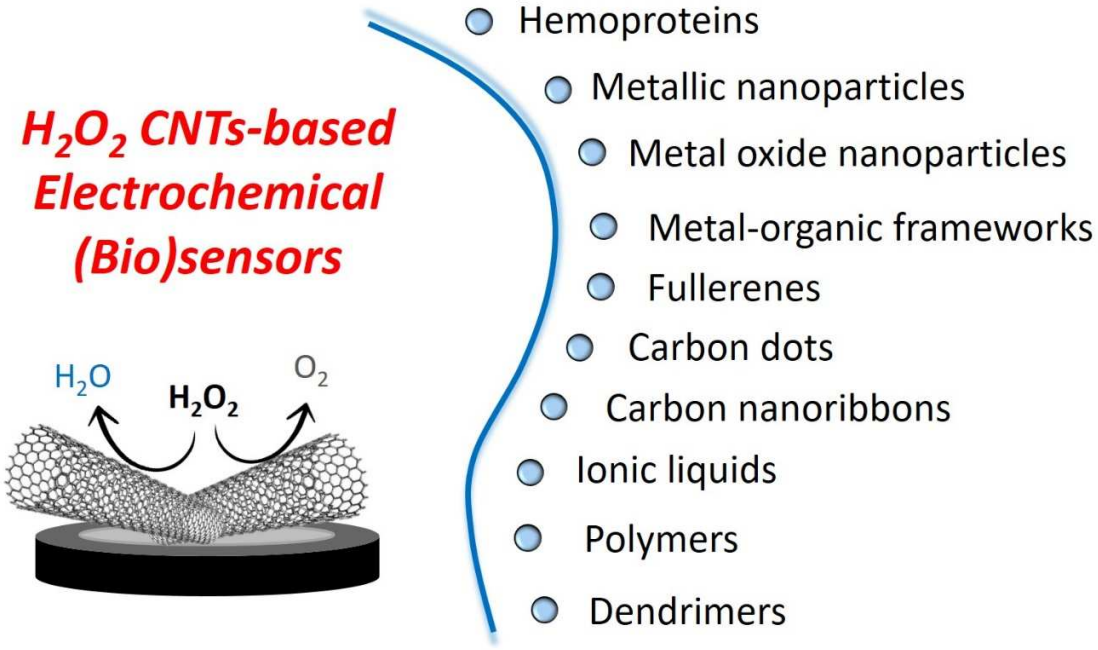

Figure 1. Graphical summary of the different topics discussed in the manuscript.

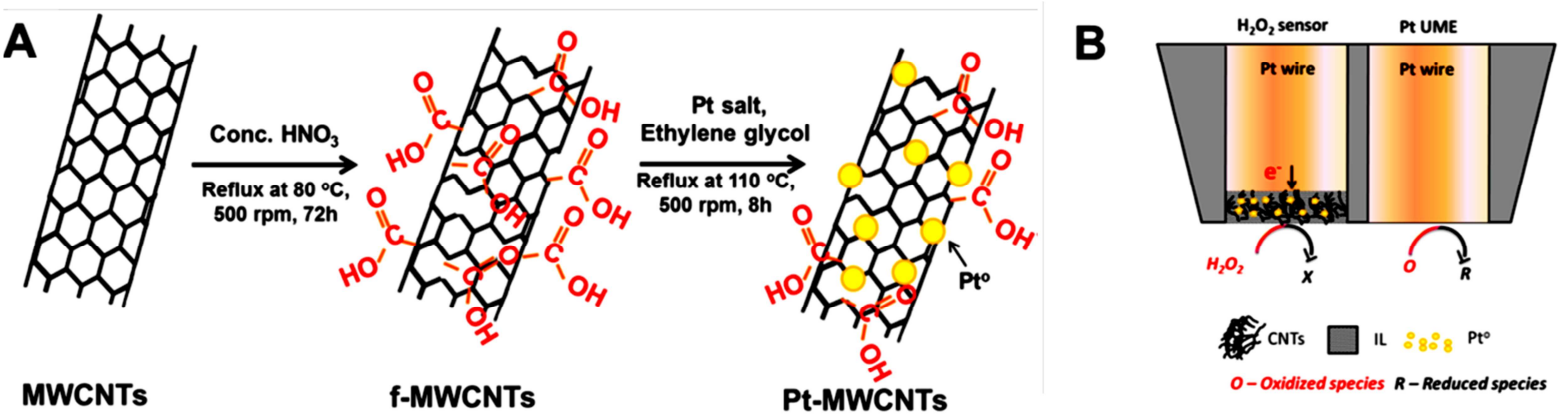

Figure 2. Schematic representation of (A) the preparation of Pt-decorated multiwalled carbon nanotubes (Pt−MWCNTs), and (B) the dual (H_2O_2 sensor/Pt) SECM probe. Adapted with permission from Ref. [35]. Copyright 2017 American Chemical Society

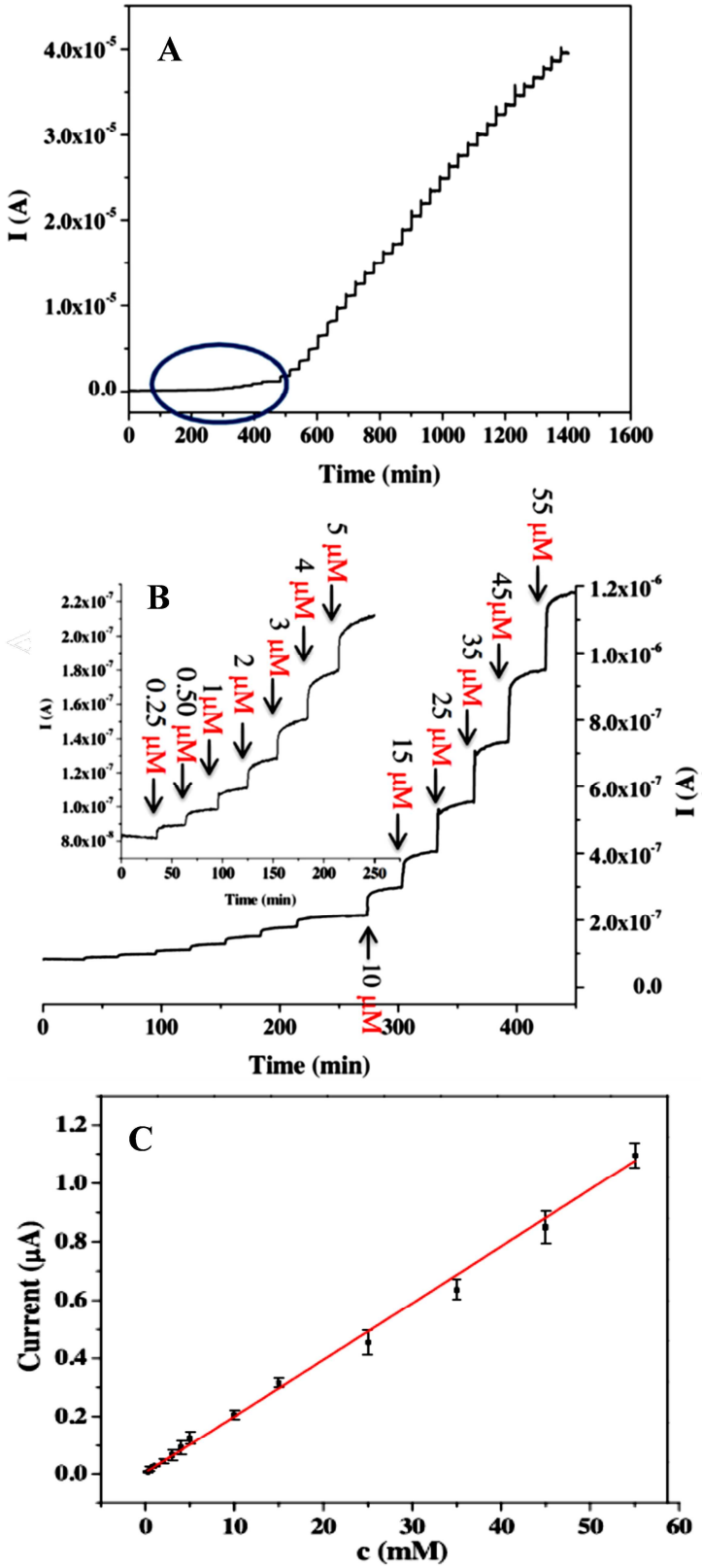

Figure 3. (A) Amperometric response at MnO_2/rGONRs/GCE for successive additions of H_2O_2. (B) Magnification of low concentration region. (C) Calibration plot obtained from the amperometric recordings shown in (B). Adapted from Ref. [46], Copyright (2017), with permission from Elsevier.

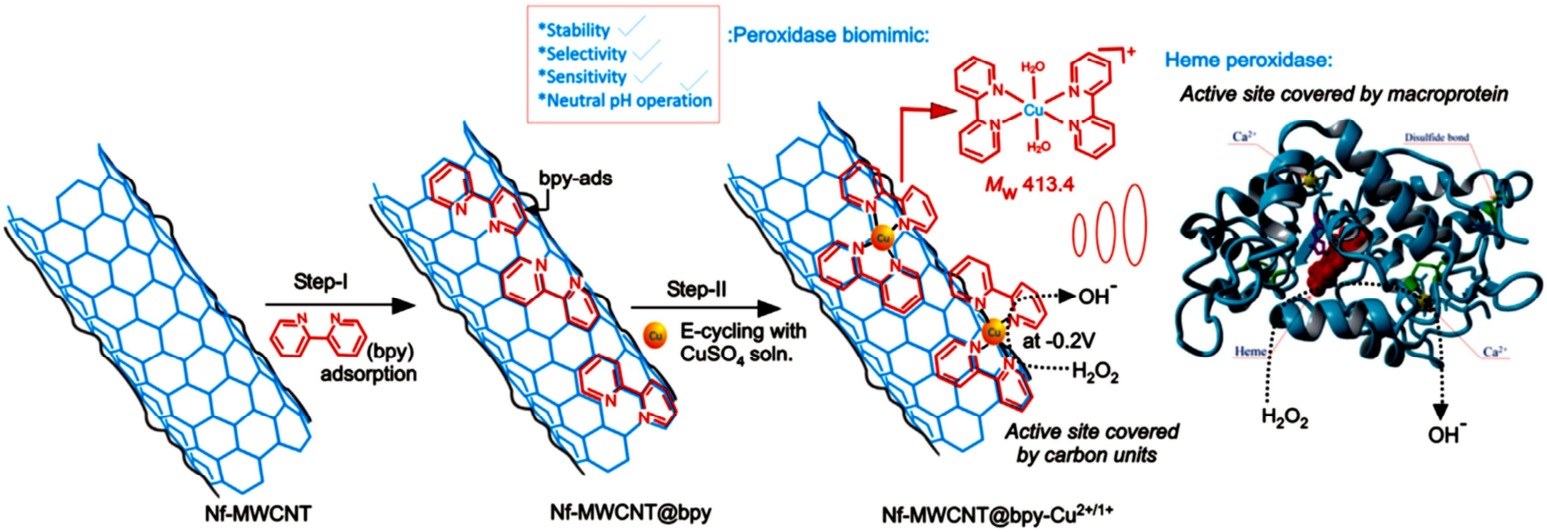

Figure 4. Scheme of the *in-situ* complexation of Cu(II) with 2,20-bipyridine(bpy) ligand immobilized Nafion(Nf)-MWCNT modified GCE and its biomimetic electrochemical reduction towards H_2O_2 at –0.2 V in neutral pH. Reprinted from Ref. [55], Copyright (2017), with permission from Elsevier.